Inorg. Chem. **2003**, *42*, 6008–6014

A Luminescent Supermolecule with Gold(I) Quinoline-8-thiolate: Crystal Structure, Spectroscopic and Photophysical Properties

Biing-Chiau Tzeng,*,† Hsien-Te Yeh,† Yung-Chi Huang,† Hsiu-Yi Chao,† Gene-Hsiang Lee,‡ and Shie-Ming Peng‡

Department of Chemistry and Biochemistry, National Chung Cheng University, 160 San-Hsin, Min-Hsiung, Chia-Yi, Taiwan 621, and Department of Chemistry, National Taiwan University, Taipei, Taiwan

Received January 15, 2003

The trinuclear complex $[(8\text{-QNS})_2Au(AuPPh_3)_2]\cdot BF_4$ (8-QNS = quinoline-8-thiolate), with intramolecular gold(I)···gold(I) distances of 3.0952(4) and 3.0526(3) Å, is aggregated to form a novel hexanuclear supermolecule, $\{[(8\text{-QNS})_2Au(AuPPh_3)_2]\}_2\cdot(BF_4)_2$, via a close intermolecular gold(I)···gold(I) contact of 3.1135(3) Å. The beautiful hexanuclear supermolecule has an inversion center, and the six metal centers can be viewed as roughly coplanar. Six gold(I) ions are embedded in an ellipse and surrounded by 4 quinoline and 12 phenyl rings. The title compound shows interesting spectroscopic and luminescence properties dependent on the solvent polarity; i.e., it emits at ca. 440 and 636 nm in CH_2Cl_2 and only at ca. 450 nm in CH_3CN. The long-lived emission at ca. 636 nm (16.2 μs) in CH_2Cl_2 is quenched by polar solvents such as CH_3CN and CH_3OH with quenching constants as 1.00×10^5 and 3.03×10^4 s^{-1} M^{-1}, respectively, which is suggested to be related to the presence or absence of gold(I)···gold(I) interactions due to scrambling of the $[AuPPh_3]^+$ units, isolobal to H^+.

Introduction

Gold(I) thiolates are the most extensively used gold(I) complexes in medicine and in surface technology.[1,2] Virtually all of the classical and modern drugs based on gold(I) for arthritis and rheumatism have been gold(I)−sulfur compounds.[3−5] The pastes known as "liquid gold" used for gold-plating of glass and ceramics are mixtures of gold(I) thiolates derived from natural products. Furthermore, precursors of advanced gold thin film technology are still relying mainly on the special properties of the gold(I)−sulfur system.[6] Surprisingly, it is only recently that major progress has been made regarding the full characterization of specific gold(I) thiolates.[7] Most of the research leading to new gold(I) aggregates with interstitial metalloid elements was initiated by following the "aurophilicity principle"[8] and also intrigued both theoretical and experimental chemists.[9−17]

The study of the solvent and/or medium effects on gold(I)···gold(I) interactions may pave the way for molecular

* To whom correspondence should be addressed. E-mail: chebct@ccu.edu.tw.
† National Chung Cheng University.
‡ National Taiwan University.

(1) (a) Parish, R. V. *Int. Sci. Rev*. **1992**, *17*, 221. (b) Sadler, P. J. *J. Adv. Inorg. Chem*. **1991**, *36*, 1.
(2) Rapson, W. S. *Gold Usage*; Academic Press: London, 1978.
(3) Brown, D. H.; Smith, W. E. *Chem. Soc. Rev*. **1980**, *9*, 217.
(4) Dash, K. C.; Schmidbaur, H. *Metal Ions in Biological Systems*; Siegel, H., Ed.; Marcel Dekker: New York 1982; Vol. 14, p 179.
(5) Sutton, B. M. *Gold Bull*. **1986**, *19*, 15.
(6) Hunt, L. B. *Gold Bull*. **1979**, *12*, 116.
(7) (a) Jones, W. B.; Yuan, J.; Narayanaswamy, R.; Young, M. A.; Elder, R. C.; Bruce, A. E.; Bruce, M. R. M. *Inorg. Chem*. **1995**, *34*, 1996. (b) Narayanaswamy, R.; Young, M. A.; Parkhurst, E.; Ouellette, M.; Kerr, M. E.; Ho, D. M.; Elder, R. C.; Bruce, A. E.; Bruce, M. R. M. *Inorg. Chem*. **1993**, *32*, 2506.
(8) (a) Schmidbaur, H. *Gold Bull*. **1990**, *23*, 11. (b) Schmidbaur, H.; Scherbaum, F.; Huber, B.; Müller, G. *Angew. Chem., Int. Ed. Engl*. **1988**, *27*, 419. 2. (c) Schmidbaur, H. *Chem. Soc. Rev*. **1995**, *24*, 391. (d) Schmidbaur, H. *Interdiscipl. Sci. Rev*. **1992**, *17*, 213. (e) Schmidbaur, H. *Gold Bull*. **2000**, *33*, 1. (f) *Gold-Progress in Chemistry, Biochemistry and Technology*; Schmidbaur, H., Ed.; John Wiley & Sons: Chichester, U.K., 1999.
(9) (a) Schneider, W.; Bauer, A.; Schmidbaur, H. *Organometallics* **1996**, *15*, 5445. (b) Hollatz, C.; Schier, A.; Schmidbaur, H. *J. Am. Chem. Soc*. **1997**, *119*, 8115. (c) Tzeng, B.-C.; Schier, A.; Schmidbaur, H. *Inorg. Chem*. **1999**, *38*, 3978.
(10) (a) Pyykkö, P. *Chem. Rev*. **1997**, *97*, 597. (b) Pyykkö, P.; Zhao, Y. *Angew. Chem., Int. Ed. Engl*. **1995**, *34*, 1894. (c) Pyykkö, P.; Li, J.; Runeberg, N. *Chem. Phys. Lett*. **1994**, *218*, 133. (d) Pyykkö, P.; Zhao, Y. *Chem. Phys. Lett*. **1991**, *177* 103. (e) Rösch, N.; Görling, A.; Ellis, D. E.; Schmidbaur, H. *Angew. Chem., Int. Ed. Engl*. **1989**, *28*, 1357. (f) Burdett, J. K.; Eisenstein, O.; Schweizer, W. B. *Inorg. Chem*. **1994**, *33*, 3261.
(11) (a) Fackler, J. P., Jr. *Polyhedron* **1997**, *16*, 1. (b) Fackler, J. P., Jr. *Inorg. Chem*. **2002**, *41*, 6959.
(12) (a) Puddephatt, R. J. *Coord. Chem. Rev*. **2001**, *216−217*, 313. (b) Puddephatt, R. J. *Chem. Commun*. **1998**, 1055. (c) Puddephatt, R. J. *The Chemistry of Gold*; Elsevier: Amsterdam, 1978.

10.1021/ic034041i CCC: $25.00
Published on Web 08/16/2003

self-assembly of gold(I) ions leading to the formation of novel gold(I) supermolecules.[17] This is particularly important for understanding the chemistry of gold(I) drugs,[18] where such interactions might occur under biological conditions. The presence of aurophilic contacts may be recognized not only from short gold(I)···gold(I) distances and novel structural features but also intriguing electronic absorption and luminescence properties.[19] It is becoming clear that the gold(I)···gold(I) bonding interaction is responsible for the relevant transitions, and luminescence has thus become an important diagnostic tool for aurophilicity. Recently, a spectacular experiment carried out by Balch et al.[13a] has demonstrated that luminescence of gold(I) complexes can be triggered by the solvation of the donor-free solid substrate either from the vapor phase or by dissolving the material in a solvent. An unusual chromic luminescence behavior linked to a structural change in the solid state induced by exposure to the vapor phase of volatile organic compounds (VOCs) was also observed by Eisenberg and co-workers.[20] The "luminescent switch" for the detection of VOCs using gold(I) dimers following the pioneering work by Mann and co-workers[21] on absorption and emission spectra of vapochromic platinum(II) and palladium(II) compounds shows that the phenomena of these kinds of luminescent gold(I) compounds hold great potential for analytical applications.

A remarkable example of the strong solvent dependence of the luminescence of a gold(I) compound in solution has been previously communicated by Che et al.[22] The quenching of the luminescence of the simple dinuclear gold(I) quinoline-8-thiolate in polar solvents such as CH_3CN and CH_3OH is attributed to an equilibrium between two forms **1A** and **1B** of the complexes (Scheme 1) of which only the former displays emission. Herein is described the molecular structures and photophysical properties of a novel complex, $[(8\text{-QNS})_2Au(AuPPh_3)_2]\cdot BF_4$, **2**·$BF_4$, isolated from a proposed rearrangement reaction of **1**·BF_4. This huge gold(I) cluster shows interesting spectroscopic and luminescence properties dependent on the solvent polarity as those in **1**·BF_4, which is suggested to be related to the presence or absence of gold(I)···gold(I) bonding interactions due to scrambling of the $[AuPPh_3]^+$ units, isolobal to H^+.

Scheme 1

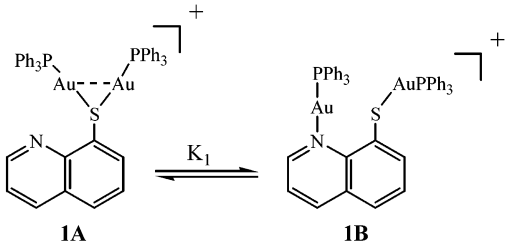

1A **1B**

Experimental Section

General Information. All reactions were performed under a nitrogen atmosphere and solvents for syntheses (analytical grade) were used without further purification. NMR: Bruker DPX 400 MHz NMR; deuterated solvents with the usual standards. MS: Positive ion FAB mass spectra were recorded on a Finnigan MAT95 mass spectrometer. Quinoline-8-thiol (8H-QNS) was purchased from Aldrich Chemicals, and Au(PPh_3)Cl was prepared by literature methods.[23] Solvents for photophysical studies were purified by literature methods.

Synthesis of $[(8\text{-QNS})_2Au(AuPPh_3)_2]\cdot BF_4$ 2·BF_4. A solution of Na(8-QNS) was prepared by adding NaOMe (30 mg) to 8H-QNS (50 mg) in CH_2Cl_2/CH_3OH (1:1, 25 mL). Au(PPh_3)Cl (250 mg, 25 mL in CH_2Cl_2) was then added to the solution, which was stirred for 4 h at room temperature. After the addition of $NaBF_4$ (60 mg), the pale yellow solution was stirred for another 10 min and then evaporated to dryness. The resulting solid was extracted with THF and then layered with hexanes. Pale-yellow single crystals were obtained in 55% yield in 1 week. MS (FAB): $[(8\text{-QNS})(AuPPh_3)_2]^+$, $m/e = 1080$, 100%; $[(8\text{-QNS})_2Au(AuPPh_3)_2]^+$, $m/e = 1436$, 10%. $\{^1H\}^{31}P$ NMR ($CDCl_3$, 25 °C): δ 33.75 (s). Anal. Calcd for $Au_3C_{54}H_{42}N_2S_2P_2BF_4$: C, 42.56; H, 2.76; N, 1.84. Found: C, 43.01; H, 2.92; N, 1.52.

Physical Measurements and Instrumentation. UV/vis spectra were recorded on a Perkin-Elmer Lambda 19 spectrophotometer, and steady-state emission spectra, on a SPEX Fluorolog-2 spectrophotometer. Emission lifetime measurements were performed with a Quanta Ray DCR-3 Nd:YAG laser (pulse output 355 nm, 8 ns). The decay signal was recorded by a R928 PMT (Hamamatsu), which was connected to a Tektronix 2430 digital oscilloscope. Solutions

(13) (a) Vickery, J. C.; Olmstead, M. M.; Fung, E. Y.; Balch, A. L. *Angew. Chem., Int. Ed. Engl.* **1997**, *36*, 1179. (b) Vickery, J. C.; Balch, A. L. *Inorg. Chem.* **1997**, *36*, 5978. (c) Calcar, P. M. V.; Olmstead, M. M.; Balch, A. L. *Inorg. Chem.* **1997**, *36*, 5231. (d) Calcar, P. M. V.; Olmstead, M. M.; Balch, A. L. *J. Chem. Soc., Chem. Commun.* **1995**, 1773.

(14) (a) Contel, M.; Garrido, J.; Gimeno, M. C.; Jones, P. G.; Laguna, A.; Laguna, M. *Organometallics* **1996**, *15*, 4939. (b) Gimeno, M. C.; Laguna, A. *Chem. Rev.* **1997**, *97*, 511. (c) Jones, P. G.; Ahrens, B. *New J. Chem.* **1998**, 104. (d) *Chem. Ber./Recueil* **1997**, *130*, 1813. (e) Vicente, J.; Chicote, M.-T.; Abrisqueta, M.-D.; Guerrero, R.; Jones, P. G. *Angew. Chem., Int. Ed. Engl.* **1997**, *36*, 1203.

(15) (a) Mingos, D. M. P.; Yau, J.; Menzer, S.; Williams, D. J. *Angew. Chem., Int. Ed. Engl.* **1995**, *34*, 1894. (b) Mingos, D. M. P. *J. Chem. Soc., Dalton Trans.* **1996**, 561.

(16) (a) Yam, V. W.-W.; Lo, K. K.-W. *Chem. Soc. Rev.* **1999**, *28*, 323. (b) Yam, V. W.-W.; Cheng, E. C.-C. *Angew. Chem., Int. Ed.* **2000**, *39*, 4240. (c) Yam, V. W.-W.; Cheng, E. C.-C. *Gold Bull.* **2001**, *34*, 20.

(17) (a) Tzeng, B.-C.; Lo, W.-C.; Che, C.-M.; Peng, S.-M. *Chem. Commun.* **1996**, 181. (b) Tzeng, B.-C.; Cheung, K.-K.; Che, C.-M. *Chem. Commun.* **1996**, 1681. (c) Tzeng, B.-C.; Che, C.-M.; Peng, S.-M. *J. Chem. Soc., Dalton Trans.* **1996**, 1769. (d) Tzeng, B.-C.; Che, C.-M.; Peng, S.-M. *Chem. Commun.* **1997**, 1771.

(18) (a) Shaw, C. F., III; Coffer, M. T.; Klingbeil, J.; Mirabelli, C. K. *J. Am. Chem. Soc.* **1988**, *110*, 729. (b) Coffer, M. T.; Shaw, C. F., III; Eidsness, M. K.; Watkins, J. W., II; Elder, R. C. *Inorg. Chem.* **1986**, *25*, 333. (c) Isab, A. A.; Sadler, P. J. *J. Chem. Soc., Dalton Trans.* **1982**, 135.

(19) (a) Che, C.-M.; Kwong, H.-L.; Yam, V. W.-W.; Cho, K.-C. *J. Chem. Soc., Chem. Commun.* **1989**, 885. (b) King, C.; Wang, J. C.; Khan, M. N. I.; Fackler, J. P., Jr. *Inorg. Chem.* **1989**, *28*, 2145. (c) Fu, W.-F.; Chan, K.-C.; Miskowski, V. M.; Che, C.-M. *Angew. Chem., Int. Ed.* **1999**, *38*, 2783.

(20) Mansour, M. A.; Connick, W. B.; Lachicotte, R. J.; Gysling, H. J.; Eisenberg, R. *J. Am. Chem. Soc.* **1998**, *120*, 1329.

(21) Exstrom, C. L.; Sowa, J. R., Jr.; Daws, C. A.; Janzen, D.; Moore, G. A.; Stewart, F. F.; Mann, K. R. *Chem. Mater.* **1995**, *7*, 15.

(22) Tzeng, B.-C.; Chan, C.-K.; Cheung, K.-K.; Che, C.-M.; Peng, S.-M. *Chem. Commun.* **1997**, 135.

(23) Schmidbaur, H.; Wohlleben, A.; Wagner, F.; Orama, O.; Huttner, G. *Chem. Ber.* **1977**, *110*, 1748.

Table 1. Crystallographic Data for **2**·BF_4

	2·BF_4
empirical formula	$C_{110}H_{92}Au_6B_2F_8N_4O_2P_4S_4$
fw	3109.42
cryst system	triclinic
space group (No.)	$P\bar{1}$(2)
a (Å)	11.5200(5)
b (Å)	15.2049(6)
c (Å)	16.7176(7)
α (deg)	72.1283(8)
β (deg)	85.2163(9)
γ (deg)	79.0915(9)
V (Å^3), *Z*	2735.6(2), 1
ρ_{calc} (g cm^{-3})	1.887
F(000) (e)	1476
μ(Mo Kα) (cm^{-1})	82.12
T (K)	295(2)
reflcns collcd	35 916
obsd reflcns ($F_o \geq 2\sigma(F_o)$)	12 553
refined params	618
R,[a] wR_2[b]	0.0368, 0.1017
ρ_{fin}(max/min) (e Å^{-3})	1.488/−0.931
goodness-of-fit on F^2	1.052

[a] $R = \sum||F_o| - |F_c||/\sum|F_o|$. [b] $wR_2 = \{[\sum w(F_o^2 - F_c^2)^2/\sum[w(F_o^2)^2]\}^{1/2}$.

for photophysical experiments were degassed by at least four freeze−pump−thaw cycles.

X-ray Crystallography. A pale-yellow crystal of approximately 0.25 × 0.25 × 0.20 mm^3 was mounted on a glass capillary. Data collection was carried out on a Bruker SMART CCD diffractometer with Mo radiation at low temperature. A preliminary orientation matrix and unit cell parameters were determined from 3 runs of 15 frames each, each frame corresponding to 0.3° scan in 15 s, followed by spot integration and least-squares refinement. Data were measured using an *ω* scan of 0.3°/frame for 20 s until a complete hemisphere had been collected. Cell parameters were retrieved using SMART[24] software and refined with SAINT[25] on all observed reflections. Data reduction was performed with the SAINT software and corrected for Lorentz and polarization effects. Absorption corrections were applied with the program SADABS.[26] The structure was solved by direct methods with the SHELX93[27] program and refined by full-matrix least-squares methods on F^2 with SHEXLTL-PC V 5.03.[27] All non-hydrogen atomic positions were located in difference Fourier maps and refined anisotropically. The hydrogen atoms were placed in their geometrically generated positions. Detailed data collection and refinement of the complex are summarized in Table 1.

Results and Discussion

Owing to the versatility of the coordination modes of quinolinethiolate such as monodentate (through S donor), bidentate (μ_2-bridging and/or chelate through S and N donors), and tridentate (μ_3-bridging through S and N donors), interesting metal thiolate clusters or supermolecules can be formed easily. In addition to the novel structural properties, the rich electrooptical properties related to visible photoluminescence arising from S → Au charge-transfer excitation can also be anticipated. The preliminary result regarding solvent effects on the spectroscopic and photophysical properties of dinuclear gold(I) quinoline-8-thiolate (**1**·BF_4) is striking,[22] and it prompted us to continue to explore the study about structural chemistry on the basis of aurophilic interactions and potential chemosensing applications. In this work, the novel supramolecular structure of **2**·BF_4 has been characterized and interesting solvent effects on spectroscopic and photophysical properties as those in **1**·BF_4 also studied.

Description of Crystal Structure. The structure of complex **2** cation shown in Figure 1(a) features a trinuclear gold(I) complex with two intramolecular gold(I)···gold(I) distances of 3.0952(4) and 3.0526(3) Å, which are further aggregated to form a novel hexanuclear supermolecule, $\{[(8\text{-QNS})_2Au(AuPPh_3)_2]\}_2\cdot(BF_4)_2$ shown in Figure 1(b), through a close intermolecular gold(I)···gold(I) contact of 3.1135(3) Å. The beautiful hexanuclear supermolecule has an inversion center, and the six metal centers can be viewed as roughly coplanar as shown in Figure 1(c). The least-square plane is calculated from the six gold ions with deviations from the plane as follows: −0.1364 Å, Au(1); 0.3350 Å, Au(2); 0.0469 Å, Au(3); 0.1364 Å, Au(1A); −0.3351 Å, Au(2A); −0.0468 Å, Au(3A). Six gold(I) ions are embedded in an ellipse and surrounded by 4 quinoline and 12 phenyl rings. There are six significant aurophilic interactions (3.0526(3)−3.1135(3) Å) in this supermolecule, which are expected to stabilize this novel supramolecular structure in the solid state. The structure can be inferred from Scheme 2 that two molecules of **1**·BF_4 underwent a proposed rearrangement (discussed in the following section) to lead to the formation of trinuclear complex **2**·BF_4 by loss of one $Au(PPh_3)_2^+$ cation. In **1**·BF_4, 8-QNS is bonded to two nearly equivalent $[AuPPh_3]^+$ units through the sulfur atom. The central gold(I) ion (isolobal to H^+) in complex **2** cation acts as a bridge between two sulfur atoms of 8-QNS($AuPPh_3$) with an almost linear S(1)−Au(2)−S(2) (174.84(6)°) bond and two different P(1)−Au(1)−S(1) (156.91(6)°) and P(2)−Au(3)−S(2) (171.52(6)°) bonds. The difference of 14.6° between the two P−Au−S moieties may be only due to the steric constraint or structural packing in the solid state. It is noted that there are two Au···N interactions in the structure. The Au(1)···N(1) distance of 2.555 Å is quite shorter than the Au(3)···N(2) distance of 3.274 Å, where the former is indicative of a strong bonding interaction and the latter is a weak one. The hexanuclear gold(I) supermolecule may be regarded as an ellipse, which is surrounded with 4 quinoline and 12 phenyl rings. Thus, we guess the surrounding quinoline and phenyl rings outside the Au_6 core possibly make this supramolecular structure flexible due to the possible rotation of C−S or C−C single bonds of the quinoline and phenyl rings, and this is in accordance with the shorter lifetime and lower quantum yield of **2**·BF_4 compared to those in **1**·BF_4.

(24) *SMART V 4.043 Software for the CCD Detector System*; Siemens Analytical Instruments Division: Madison, WI, 1995.
(25) *SAINT V 4.035 Software for the CCD Detector System*; Siemens Analytical Instruments Division: Madison, WI, 1995.
(26) Sheldrick, G. M. *SHELXL-93, Program for the Refinement of Crystal Structures*; University of Gottingen: Gottingen, Germany, 1993.
(27) *SHELXTL 5.03 (PC-Version), Program Liberary for Structure Solution and Molecular Graphics*; Siemens Analytical Instruments Division: Madison, WI, 1995.

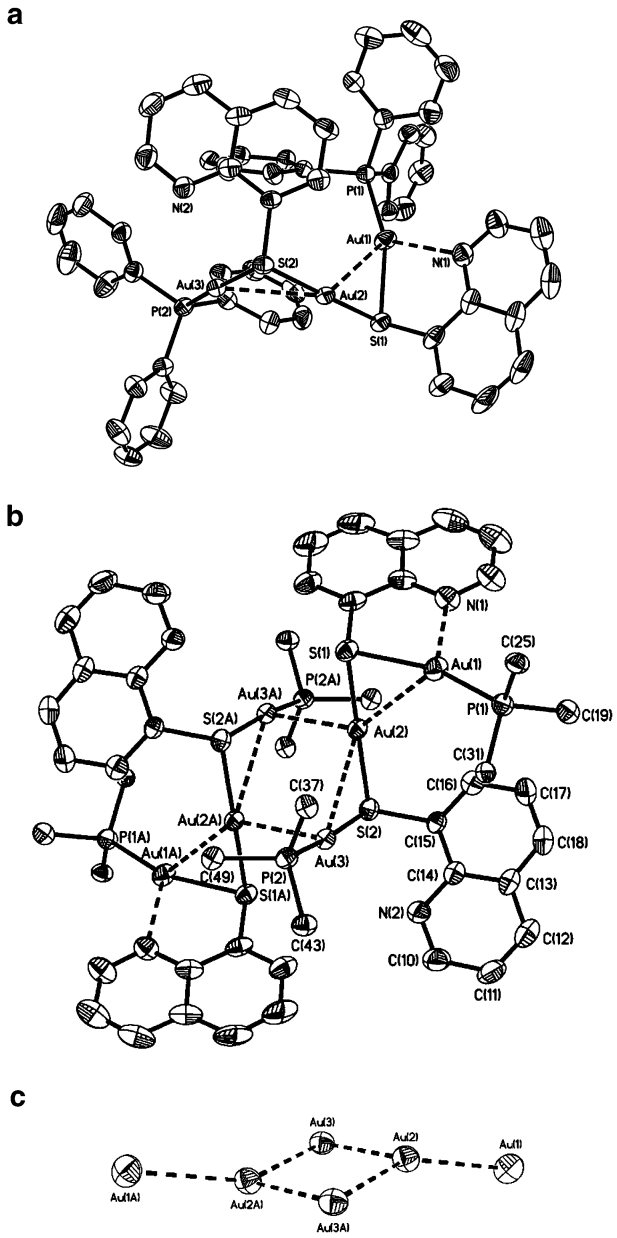

Figure 1. (a) Perspective view of complex **2** cation (bond lengths in Å, angles in deg): Au(1)···Au(2) 3.0952(4), Au(2)···Au(3) 3.0526(3), Au(1)−S(1) 2.3789(16), Au(2)−S(2) 2.3188(16), Au(3)−S(2) 2.3502(16), Au(1)−P(1) 2.2420(16), Au(3)−P(2) 2.2633(16); S(1)−Au(1)−P(1) 156.91(6), S(1)−Au(2)−S(2) 174.84(6), S(2)−Au(3)−P(2) 171.52(6). (b) Dimeric aggregate of complex **2** cations leading to the formation of a hexanuclear gold(I) supermolecule connected by intermolecular Au(2)···Au(3A) contact of 3.1135(3) Å. For clarity only the ipso carbons of the phenyl rings are shown. (c) The six metal centers can be viewed as roughly coplanar.

UV−Visible Absorption and Emission Spectra. The absorption spectra of **2**·BF_4 measured in CH_2Cl_2, $CHCl_3$, THF, CH_3OH, and CH_3CN are shown in Figure 2. Table 2 summarizes the spectroscopic and photophysical data of **2**·BF_4 in various solvents. It is somewhat surprising that although **2**·BF_4 is a huge structure, its absorption spectra measured in the same solvent are almost identical to those of dinuclear **1**·BF_4, except the latter has weaker absorptions. There is a distinct difference in the absorption spectra of **2**·BF_4 measured in CH_2Cl_2 and in CH_3CN. In CH_2Cl_2, this complex shows an intense absorption band at ca. 320 nm,

Scheme 2

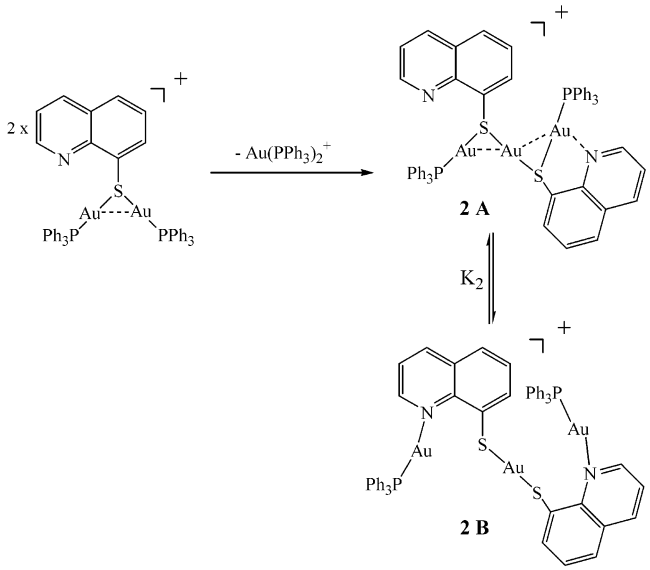

whereas there is a weaker absorption band at ca. 320 nm as well as an additional absorption band at ca. 380 nm in CH_3CN. The absorption spectra measured in $CHCl_3$, THF, and CH_3OH are quite similar to that measured in CH_2Cl_2, except with a low-energy absorption band at ca. 400 nm measured in THF. This low-energy absorption is red-shifted to the above measured in CH_3CN, and the red shift is also observed in **1**·BF_4. In the inset of Figure 2, the spectral change with two isosbestic points at 357 and 366 nm shows a decrease in the absorption at ca. 320 nm concomitant with an increase in the absorption at ca. 380 nm upon addition of CH_3CN to a CH_2Cl_2 solution of **2**·BF_4. The absorption at ca. 380 nm of **2**·BF_4 measured in CH_3CN strongly resembling in that of [8-QNS($AuPPh_3$)] (ca. 386 nm) as well as that in **1**·BF_4 (ca. 386 nm) measured in CH_3CN is tentatively assigned to an intraligand transition of thiolates and/or a S → Au charge-transfer transition. Indeed, the absorption spectra measured in CH_2Cl_2, $CHCl_3$, and CH_3OH also show a very weak absorption in this spectral range. Notably, the absorption at ca. 320 nm of **2**·BF_4 is similar to that in **1**·BF_4 and is also in energy relative to the low-energy 5d($d\sigma^*$) → 6p($p\sigma$) transitions in a number of dinuclear and trinuclear gold(I) phosphine complexes such as $[Au_2(dppm)_2]^{2+}$ (295 nm)[28] and $[Au_3(dpmp)_2]^{3+}$ (326 nm).[29] This may be a major difference between the forms in Schemes 1 and 2 (discussed in the following section) with or without gold(I)···gold(I) interactions, as reflected by the presence or absence of the absorption at ca. 320 nm. However, none of the spectra exclusively shows only one absorption band at ca. 320, suggesting that there is no pure isomeric form of **2**·BF_4 (with or without gold(I)···gold(I) interactions) in the solutions but a mixture at an equilibrium. Surprisingly, the huge complex structure of **2**·BF_4 with six gold(I) ions connected by six significant aurophilic interactions in the solid state leading

(28) Che, C.-M.; Kwong, H.-L.; Poon, C.-K.; Yam, V. W.-W. *J. Chem. Soc., Dalton Trans.* **1990**, 3215.
(29) Li, D.; Che, C.-M.; Peng, S.-M.; Liu, S.-T.; Zhou, Z.-Y.; Mak, T. C.-W *J. Chem. Soc., Dalton Trans.* **1993**, 189.

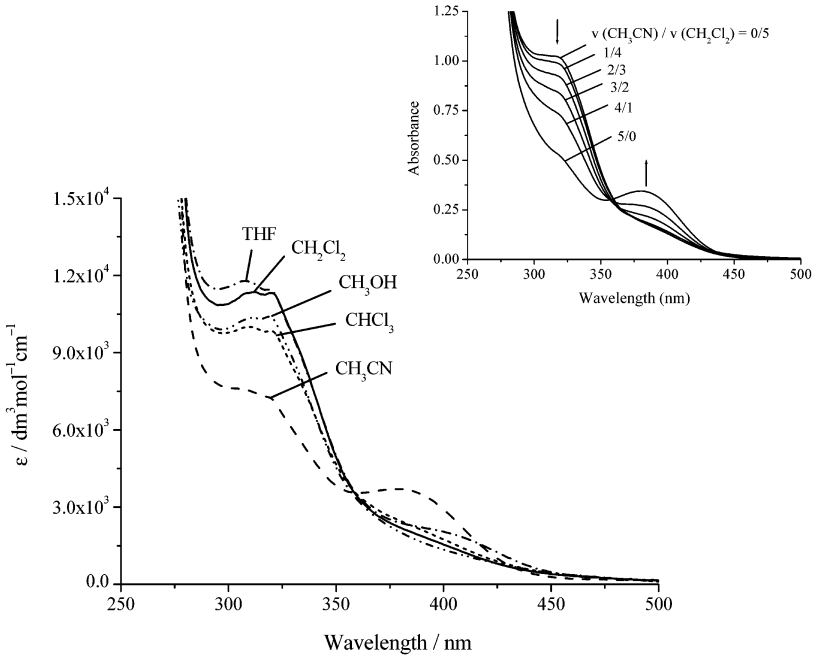

Figure 2. Electronic absorption spectra of **2**·BF_4 measured in various solvents (CH_2Cl_2, $CHCl_3$, THF, CH_3OH, and CH_3CN) at 298 K. Inset is the spectral change upon addition of CH_3CN to a CH_2Cl_2 solution (9×10^{-5} M) with a v (CH_3CN)/v (CH_2Cl_2) ratio from 0/5, 1/4, 2/3, 3/2, 4/1, to 5/0 leading to a decrease in the absorption at ca. 320 nm concomitant with an increase in the absorption at ca. 386 nm when the CH_3CN content increases.

Table 2. Spectroscopic and Photophysical Data for **2**·BF_4

solvents	λ_{abs} (nm)/ ϵ ($dm^3\ mol^{-1}\ cm^{-1}$)	λ_{em} (nm)/τ (μs) solution	λ_{em} (nm)/τ (μs) solid state (RT)	k_q ($s^{-1}\ M^{-1}$)
			587/27.4	
			(510, 545, 590/283.7)[a]	
CH_2Cl_2	320/11 310	440/0.8		
	(320/8060)[a]	(430/0.3)[a]		
	380/2180	636/16.2		
	(386/230)[a]	(640/26.0)[a]		
$CHCl_3$	320/9840	425/0.7		1.10×10^3
	380/2460	636/11.3		
THF	320/11 420	425/0.7		1.84×10^4
	400/2040	636/2.5		(3.2×10^4)[a]
CH_3OH	320/10 390	425/0.7		3.03×10^4
	380/1,960	636/1.8		(5.0×10^4)[a]
CH_3CN	320/7260	450/0.7		1.00×10^5
	(320/5870)[a]	(440/0.3)[a]		(1.25×10^5)[a]
	380/3710			
	(386/1450)[a]			

[a] Data in parentheses represent the related values of **1**·BF_4.

to the formation of a supramolecular structure also shows a proposed scrambling of $[Ph_3PAu]^+$ units in polar solvents.

The solid-state emission spectra of **2**·BF_4 measured in CH_2Cl_2, $CHCl_3$, THF, CH_3OH, and CH_3CN at room temperature are shown in Figure 3. For a purpose of comparison, the solid-state emission spectrum of **1**·BF_4 is also included. At room temperature and in the solid state, complex **2**·BF_4 displays a red-orange emission at ca. 587 nm with a lifetime of 27.4 μs upon photoexcitation at 355 nm, whereas **1**·BF_4 shows a bright yellow and vibronic-structured emission with peak maxima at ca. 508, 545, and 590 nm with a lifetime of 283.7 μs. This progression with a spacing at 1300−1400 cm^{-1} is mostly due to the C═C or C═N stretching mode of the 8-QNS ligand, and the emission is most likely due to a S → Au excitation and possibly with modification of gold(I)···gold(I) interactions. The correlation between the emission energy and the gold(I)···gold(I) interaction was studied by Fackler and co-workers[30] on a series of monomeric gold(I) complexes containing phosphine and thiolate (aromatic) ligands. All of the compounds synthesized by Fackler et al. luminesce at 77 K (485−702 nm) in the solid state, and the excitation was also assigned to a S → Au charge-transfer transition. According to their studies, the emission energy can be tuned either by changing the substituents on the thiolates or by the presence of gold(I)···gold(I) interactions in the solid state. Since there are six intra- and intermolecular gold(I)···gold(I) interactions for the solid-state structure of **2**·BF_4, the emission at ca. 587 nm assigned to a S → Au charge-transfer transition strongly modified by a metal-centered 5d(dσ*) → 6p(pσ) transition is anticipated.

(30) Forward, J. M.; Bohmann, D.; Fackler, J. P., Jr.; Staples, R. J. *Inorg. Chem.* **1995**, *34*, 6330.

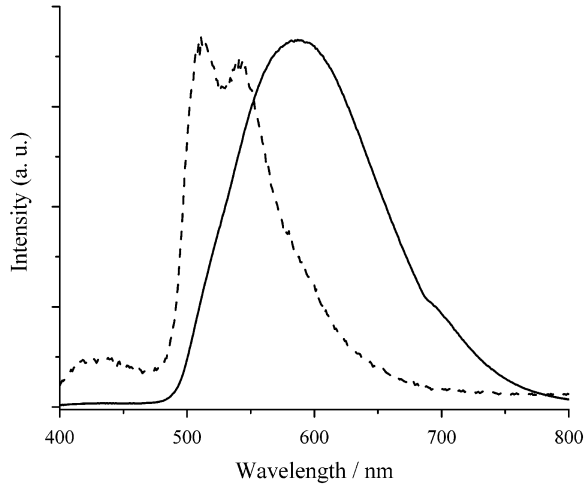

Figure 3. Solid-state emission spectra of **1**·BF_4 (dash line) and **2**·BF_4 (solid line) measured at 298 K. Excitation is at 355 nm.

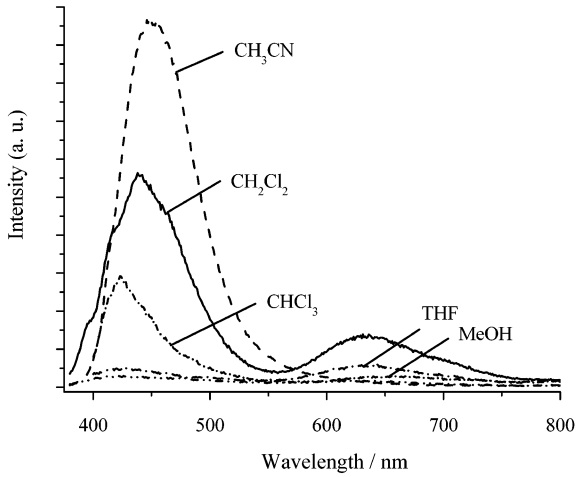

Figure 4. Emission spectra of **2**·BF_4 measured in various solvents (CH_2Cl_2, $CHCl_3$, THF, CH_3OH, and CH_3CN) at 298 K. Complex concentration = 9×10^{-5} M. Excitation is at 320 nm.

As shown in Figure 4, photoexcitation of a CH_2Cl_2 solution of **2**·BF_4 gave an intense emission at ca. 450 nm and a weak one at ca. 636 nm, and a similar emission in $CHCl_3$ was also observed. It is somewhat different from those measured in CH_2Cl_2 and $CHCl_3$ that the emission spectra measured in THF and CH_3OH show only very weak high- (ca. 424 nm) and low-energy (ca. 636 nm) emissions. However, the low-energy emission is absent upon photoexcitation of a CH_3CN solution of **2**·BF_4 with only a high-energy emission at ca. 440 nm. The low-energy emission of **2**·BF_4 measured in CH_2Cl_2 is similar to that in **1**·BF_4, except the former having a weaker emission intensity and a shorter lifetime. Because there is only a weak- and high-energy emission at ca. 477 nm for [8-QNS($AuPPh_3$)] without any aurophilic interaction, the excited state is supposed to originate from a S → Au charge-transfer transition, and an intraligand transition of the thiolate ligand cannot be excluded. On the basis of the only weak- and high-energy emission for [8-QNS($AuPPh_3$)] as well as Fackler's work, the low-energy excited state of **2**·BF_4 is tentatively assigned to a S → Au charge-transfer transition modified by a metal-centered 5d(dσ*) → 6p(pσ) transition as the solid-state excitation origin. The high-energy emissions

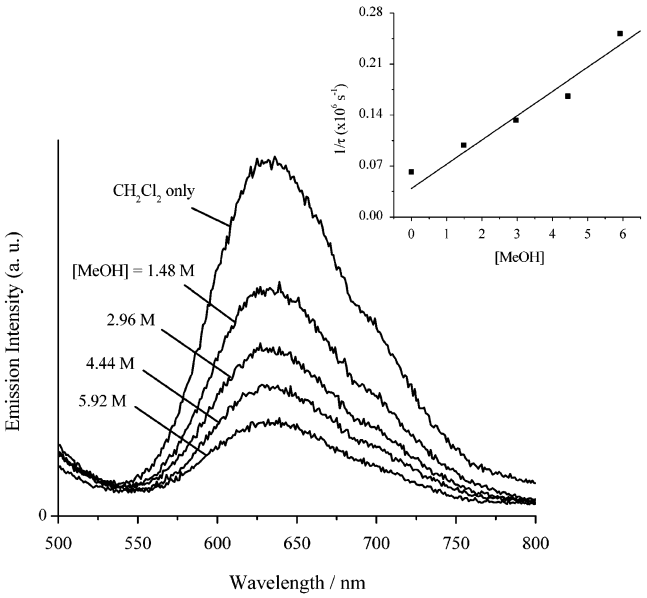

Figure 5. Representative example shows the spectral change upon addition of CH_3OH to a CH_2Cl_2 solution of **2**·BF_4 (7.72×10^{-5} M) with excitation at 320 nm. The lifetime change according to the Stern−Volmer equation is shown in the inset.

at ca. 425−450 nm are suggested to be due to an intraligand transition of PPh_3, but it should be noted that the possibility of having the emission contributed from the Au−PPh_3 portion could not be excluded, since the complex Au(PPh_3)X (X = halide) also shows photoluminescence in this spectral region.[31] Notably, these emissions depend on the solvent polarity as those in **1**·BF_4. Polar solvents such as CH_3CN, CH_3OH, THF, and $CHCl_3$ were found to quench the low-energy emissions with Stern−Volmer quenching rate constants in the order: $CH_3CN > CH_3OH > THF > CHCl_3$ ($k_q = 1.00 \times 10^5$, 3.03×10^4, 1.84×10^4, and 1.10×10^3 s^{-1} M^{-1}, respectively), which are comparable to those in **1**·BF_4. In CH_3CN, the ca. 636 nm emission virtually disappears, whereas it has the highest quantum yield (QY = 0.001) and longest lifetime ($\tau = 16.2$ μs) in CH_2Cl_2, and both are smaller than those in **1**·BF_4 (QY = 0.02, τ = 26.0 μs). In Figure 5, a representative example shows the spectral change upon addition of CH_3OH to a CH_2Cl_2 solution of **2**·BF_4, which causes emission intensities decreased and lifetimes shortened. The quenching plot is shown in the inset of Figure 5, and the quenching constant is obtained from the slope of the Stern−Volmer plot. The quenching constants of **1**·BF_4 and **2**·BF_4 are also summarized in Table 2.

In a proposed rearrangement process (Scheme 2), **2**·BF_4 is serendipitously isolated and characterized by the X-ray crystallographic and spectroscopic study. Scrambling of $AuPPh_3^+$ unit causing a structural change or isomerization is suggested to be responsible for the dramatic spectroscopic and luminescence change in various solvents with the different polarity. Scheme 1 shows an equilibrium reaction between **1A** and **1B** with the equilibrium constant K_1 (=[**1B**]/[**1A**]), where the former is supposed to have a

(31) Larson, L. J.; McCauley, E. M.; Weissbart, B.; Tinti, D. S. *J. Phys. Chem.* **1995**, *99*, 7218.

gold(I)···gold(I) interaction and the latter has none. Since there is only a weak- and high-energy emission at ca. 477 nm for [8-QNS($AuPPh_3$)], it does not show any aurophilic interaction. Thus, the gold(I)···gold(I) interaction is suggested to be responsible for the low-energy emission at ca. 640 nm for **1**·BF_4. The solvent polarity could affect the charge localization or delocalization over the 8-QNS ligand as well as the isomer formation of the **1A** (**2A**) or **1B** (**2B**) forms. The Au(I)···N interactions are anticipated to play a key role in facilitating the formation of **2B** in CH_3CN, although how the polarity influences the isomer formation is sill unclear. In an earlier communication, Che et al.[17d] reported a novel luminescent gold(I) supermolecule with trithiocyanuric acid, $[(LAu)(AuPPhMe_2)_2]_2$ (H_3L = trithiocyanuric acid), which has a novel two-dimensional framework via intermolecular gold(I)···gold(I) interactions and possesses interesting photoluminescence properties. It is unexpected that the hexanuclear supermolecule is obtained by slow diffusion of Et_2O into a CH_2Cl_2/CH_3OH solution of $[L(AuPPhMe_2)_3]$. Presumably, two trinuclear $[L(AuPPhMe_2)_3]$ molecules undergo a rearrangement process upon loss of two $PPhMe_2$ molecules to form $[(LAu)(AuPPhMe_2)_2]_2$. In a rationale based on the above example and Scheme 1, the absorption similarity between [8-QNS($AuPPh_3$)] (ca. 386 nm) and **1**·BF_4 (ca. 386 nm) or **2**·BF_4 (ca. 380 nm) measured in CH_3CN is proposed to explain the formation scheme of **2**·BF_4, shown in Scheme 2. In Scheme 2, we propose that two **1**·BF_4 molecules undergo a rearrangement process to give rise to **2**·BF_4 with loss of one $[Au(PP_3)_2](BF_4)$. **2A** shows close gold(I)···gold(I) interactions which are suggested to be responsible for the low-energy emission for **2**·BF_4. Accordingly, **2B** has no close aurophilic interaction as well as low-energy emission. K_2 (=[**2B**]/[**2A**]) represents the equilibrium reaction between **2A** and **2B**. Thus, Schemes 1 and 2 have a similar rationale to explain the dramatic solvent effect on spectroscopic and luminescence properties of both **1**·BF_4 and **2**·BF_4 dependent on the solvent polarity. However, the identification about $Au(PPh_3)_2^+$ units is still unsuccessful, but the isolated $[Au(PPh_3)Cl]$ may be obtained from $[Au(PPh_3)_2]\cdot BF_4 + Cl^- \rightarrow [Au(PPh_3)Cl] + BF_4^- + PPh_3$.

A concentration-dependence UV−vis absorption study in CH_2Cl_2 and CH_3CN has been performed. The absorption band at ca. 320 nm measured in CH_2Cl_2 obeys the Beer law in the concentration range $10^{-6}-10^{-3}$ M suggesting that no dimerization, oligomerization, or isomerization of the metal complex occurs. This is in accordance with the absorption spectrum of **2**·BF_4 measured in CH_2Cl_2, since it shows only one strong absorption band and a very weak band at ca. 380 nm. However, the absorption band at ca. 320 and 380 nm measured in CH_3CN cannot obey the Beer law in the same concentration range. This distinction of the absorption spectra may be helpful to elucidate that the species in CH_2Cl_2 is mostly in a **2A** form, responsible for the low-energy emission, and, in CH_3CN, **2A**,**B** are both present in a significant amount. Thus, the undergoing isomerization (**2A** ↔ **2B**) is most likely responsible for the distinction of absorption behavior, obeying or not obeying the Beer law, between solvents CH_2Cl_2 and CH_3CN, respectively. A self-quenching rate constant for the ca. 636 nm emission is also measured in CH_2Cl_2 as 2.88×10^8 s^{-1} M^{-1} but not show any energy change for concentration-dependence emission study in CH_2Cl_2 and CH_3CN.

Conclusion

The beautiful hexanuclear supermolecule has 6 gold(I) ions embedded in an ellipse and surrounded by 4 quinoline and 12 phenyl rings. It is somewhat surprising that although **2**·BF_4 is a huge supramolecular structure with six gold(I) atoms connected by six significant aurophilic interactions in the solid state, it still shows scrambling of $[Ph_3PAu]^+$ units. Not only is the supramolecular structure of **2**·BF_4 novel, but an interesting family of compounds containing both **1**·BF_4 and **2**·BF_4 showing a dramatic solvent effect on spectroscopic and luminescence properties dependent on the solvent polarity have also been built up. We anticipate that given this property of luminescence, gold(I) compounds could find useful applications in the future design of new luminescence sensors and molecular light-switch devices. Studies of the detection of volatile organic compounds (VOCs) using optical-fiber technology in combination with solvent-induced luminescence properties of this interesting family of compounds are in progress.

Acknowledgment. We thank the National Science Council and National Chung Cheng University of the Republic of China for financial support (NSC 90-2113-M-194-028 and 91-2113-M-194-019).

Supporting Information Available: Crystallographic data in CIF format. This material is available free of charge via the Internet at http://pubs.acs.org.

IC034041I